Journal of the National Cancer Center 5 (2025) 38–49

Contents lists available at ScienceDirect

Journal of the National Cancer Center

journal homepage: www.elsevier.com/locate/jncc

Full Length Article

Treatments of transarterial chemoembolization (TACE), stereotactic body radiotherapy (SBRT) and immunotherapy reshape the systemic tumor immune environment (STIE) in patients with unresectable hepatocellular carcinoma☆

Cai-Ning Zhao[1,2,3,†], Chi-Leung Chiang[1,3,†], Wan-Hang Keith Chiu[4,5], Sik-Kwan Kenneth Chan[3], Chun-Bong James Li[6], Wei-Wei Chen[1,3], Dan-Yang Zheng[1,3], Wen-Qi Chen[1], Ren Ji[7], Chung-Mau Lo[8], Salma K. Jabbour[9], Chi-Yan Albert Chan[8], Feng-Ming (Spring) Kong[1,3,*]

[1] *Department of Clinical Oncology, University of Hong Kong-Shenzhen Hospital, Shenzhen, China*
[2] *Chinese Academy of Sciences (CAS) Key Laboratory of Quantitative Engineering Biology, Shenzhen Institute of Synthetic Biology, Shenzhen Institutes of Advanced Technology, Chinese Academy of Sciences, Shenzhen, China*
[3] *Department of Clinical Oncology, School of Clinical Medicine, Li Ka Shing Faculty of Medicine, The University of Hong Kong, Hong Kong, China*
[4] *Department of Diagnostic Radiology, School of Clinical Medicine, Li Ka Shing Faculty of Medicine, The University of Hong Kong, Hong Kong, China*
[5] *Department of Radiology & Imaging, Queen Elizabeth Hospital, Hong Kong, China*
[6] *Department of Pediatrics and Adolescent Medicine, School of Clinical Medicine, Li Ka Shing Faculty of Medicine, The University of Hong Kong, Hong Kong, China*
[7] *Department of Surgery, University of Hong Kong-Shenzhen Hospital, Shenzhen, China*
[8] *Department of Surgery, School of Clinical Medicine, Li Ka Shing Faculty of Medicine, The University of Hong Kong, Hong Kong, China*
[9] *Department of Radiation Oncology, Rutgers Cancer Institute of New Jersey, Rutgers Robert Wood Johnson Medical School, Rutgers University, New Brunswick, USA*

ARTICLE INFO

Keywords:
Immunotherapy
Radiotherapy
Liver cancer
Biomarker
Systemic immunity

ABSTRACT

Background: The role of systemic tumor immune environment (STIE) is unclear in hepatocellular carcinoma (HCC). This study aimed to exam the cells in the STIE, their changes after transarterial chemoembolisation (TACE), stereotactic body radiotherapy (SBRT), and immunotherapy (IO) and explore their significance in the treatment response of patients with unresectable HCC.

Methods: This is a prospective biomarker study of patients with unresectable HCC. The treatment was sequential TACE, SBRT (27.5–40 Gy/5 fractions), and IO. The treatment response was assessed according to modified Response Evaluation Criteria in Solid Tumors (mRECIST) by magnetic resonance imaging (MRI) after 6 months of treatment. Longitudinal data of STIE cells was extracted from laboratory results of complete blood cell counts, including leukocytes, lymphocytes, neutrophils, monocytes, eosinophils, basophils, and platelets. Peripheral blood samples were collected at baseline and after TACE, SBRT, and IO for T-lymphocyte subtyping by flow cytometry. Generalized estimation equation was employed for longitudinal analyses.

Results: A total of 35 patients with unresectable HCC were enrolled: 23 patients in the exploratory cohort and 12 in the validation cohort. STIE circulating cells, especially lymphocytes, were heterogenous at baseline and changed differentially after TACE, SBRT, and IO in both cohorts. SBRT caused the greatest reduction of 0.7×10^9/L (95 % CI: 0.3×10^9/L–1.0×10^9/L, $P < 0.001$) in lymphocytes; less reduction was associated with significantly better treatment response. The analysis of T-lymphocyte lineage revealed that the baseline levels of $CD4^+$ T cells ($P = 0.010$), type 1 T helper (Th1) cells ($P = 0.007$), and Th1/Th17 ratios ($P = 0.001$) were significantly higher in responders, while regulatory T (Treg) cells ($P = 0.002$), Th17 cells ($P = 0.047$), and Th2/Th1 ratios ($P = 0.028$) were significantly higher in non-responders. After treatment with TACE, SBRT and IO, T-lymphocyte lineage also changed differentially. More reductions were observed in $CD25^+CD8^+$ T cells and $CD127^+CD8^+$ T cells after

☆ Given her role as Associate Editor in this journal, Feng-Ming (Spring) Kong had no involvement in the peer-review of this article and has no access to information regarding its peer-review. Full responsibility for the editorial process for this article was delegated to Mei Wang.

* Corresponding author.
E-mail address: kong0001@hku.hk (F.M.S. Kong).

† These authors contributed equally to this work.

https://doi.org/10.1016/j.jncc.2024.06.007
Received 29 December 2023; Received in revised form 22 May 2024; Accepted 12 June 2024

SBRT in non-responders, while increases in natural killer T (NKT) cells after SBRT (10.4% vs. 3.4 %, $P = 0.001$) and increases in the lymphocyte counts were noted during IO in responders.

Conclusions: STIE cells are significant for treatment response, can be reshaped differentially after TACE, SBRT, and IO. The most significant changes of T-lymphocyte lineage are SBRT associated modulations in $CD25^+CD8^+$ T cells, $CD127^+CD8^+$ T cells, and NKT cells, which also have significant effects on the ultimate treatment response after TACE-SBRT-IO (ClinicalTrails.gov identifier: GCOG0001/NCT05061342).

1. Introduction

The hepatic tumor immune microenvironment (TIME) plays an influential role in the treatment outcome of patients with hepatocellular carcinoma (HCC).[1] The immune cell subsets in TIME can be induced by tumor cells or other components in the tumor microenvironment, or derived from the circulation as part of tumor systemic immune environment (STIE). In response to treatment perturbations, STIE, beyond the TIME level, has been recently reported to react and produce dynamic changes of immune content within and across the TIME. This improved understanding of tumor immunology has stimulated a growing body of research on the systemic immune landscape beyond the local TIME.[2] Systemic T cell expansion has been considered essential for producing durable immune response, and it has been demonstrated that novel T cells were recruited into the TIME rather than reinvigoration of pre-existing tumor infiltrating lymphocytes.[3,4] Importantly, the status of STIE could infer treatment response and prognosis in multiple types of malignancies.[3,5-8] This is encouraging as longitudinal surveillance of STIE by simple blood testing could potentially serve as an ideal biological approach to providing oncologic insights during anticancer treatment.

Cancer treatment can reshape the host T-lymphocyte dominated STIE, which has subsequent effects following treatment, as we have recently reported.[2] In recent years, the interactions between anticancer therapies and STIE in HCC have attracted attention, especially to T-lymphocytes and its subtypes. For instance, an elevated level of circulating regulatory T (Treg) cells in HCC patients following transarterial chemoembolization (TACE) treatment has been reported to incur a poor cancer prognosis, while higher levels of natural killer T (NKT) and $CD25^+CD8^+$ T cells were reported to associate with improved overall survival in HCC patients following radiotherapy.[9-12] Apart from this, Chew et al. reported that the clinical benefit of HCC patients receiving Yttrium-90 radioembolization treatment was associated with increases in programmed cell death 1 (PD-1)/Tim-3 expressing $CD8^+/CD4^+$ T cells, CCR5/CXCR6 expressing $CD8^+$ T cells and $CD8^+Tim\text{-}3^+$ T cells.[12,13] Previous studies focused on single-modality treatments, which underscore the need for a comprehensive analysis of multi-modality regimens. Our phase II trial on a combined multi-modality regimen with sequential TACE and SBRT followed by IO, referred to as START-FIT (NCT03817736) had heterogenous primary results,[14] providing an opportunity of studying the changes in STIE immune cells after various treatment modalities in unresectable HCC.

We here hypothesize that STIE cells, particularly T-lymphocytes, play an important role in tumor responses to the subsequent therapy, and each treatment modality of TACE, SBRT, and IO reshapes the STIE. Specifically, we tested the lymphocytes and the T-lymphocyte subtype distribution before and after delivery of each treatment to the same patient, and aimed to study how the overall immune cells in STIE change after TACE, SBRT, and IO, and explore the effects on the ultimate treatment responses in these patients with unresectable HCC.

2. Materials and methods

2.1. Study population

This is a prospective biomarker study (GCOG0001/NCT05061342) approved by the Institutional Review Boards of Queen Mary Hospital (UW 19–565) since August 2019. All patients signed the informed consent for specimen and questionnaire collection. Patients were newly diagnosed with locally advanced HCC not suitable for curative resections and treated with multimodality therapy of TACE and SBRT followed by IO as per START-FIT trial (NCT03817736). START-FIT was a single-arm, phase 2 trial. Other eligibility criteria included tumor size ≥5 cm, number of tumor mass ≤ 3, and child-Pugh A5-B7 liver function. Patients with prior TACE, hepatic radiotherapy, or systemic treatments were excluded. Patients with distant metastasis, main portal vein (VP4) invasion, or inferior vena cava (VV3) invasion were excluded.

2.2. Treatment and study data collection

The START-FIT treatment regimen includes a single dose of conventional TACE with Cisplatin and Lipiodol, followed by 5 fractions of SBRT with dose ranging between 27.5 and 40 Gy depending on tumor volume, which encompassed 95 % of the planning target volume, and finally IO every 2 weeks (Fig. 1).

A series of potential risk factors were recorded, including patient factors (demographic factors, *Hepatitis* history, performance status, and Child Pugh score), and tumor factors (pathologic stage, number and size of tumors, and intra-hepatic vascular invasion).

Longitudinal data of STIE cells including lymphocytes were extracted from laboratory results of complete blood cell counts, along with absolute counts of leukocytes, neutrophils, monocytes, eosinophils, basophils and platelets, at baseline/Pre-TACE, post-TACE/pre-SBRT, post-SBRT/pre-IO, and post-IO.

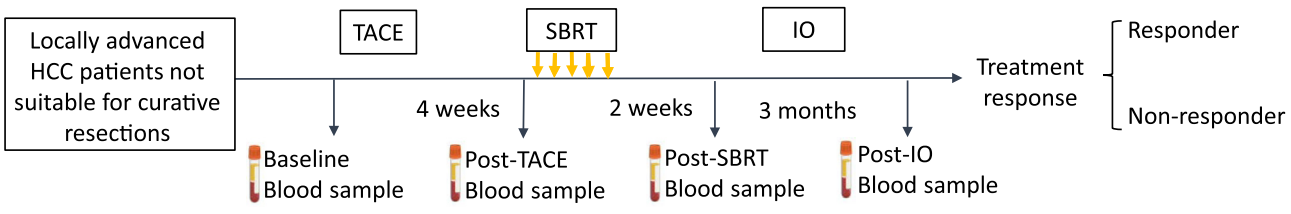

Fig. 1. The study schedule and blood sampling timepoints. HCC patients were treated with a single dose of conventional TACE, followed by 5 fractions of SBRT, and finally IO. The repeated imaging assessment was conducted every 3 months to monitor tumor size, and the treatment response was evaluated after 6 months of IO. The blood samples were collected at baseline, post-TACE, post-SBRT, and after 3 months of IO. HCC, hepatocellular carcinoma; IO, immunotherapy; SBRT, stereotactic body radiotherapy; TACE, transarterial chemoembolization.

For lymphocyte subtyping, peripheral blood samples were collected in Ethylene Diamine Tetraacetic Acid tubes at baseline/pre-TACE, post-TACE/pre-SBRT, post-SBRT/pre-IO, and post-IO for a range of circulating T cell subtypes (Fig. 1). These blood samples were collected and restored at 4 °C before the separation of buffy coat at 1600 g for 10 min. Peripheral blood lymphocytes were collected from buffy coat, frozen in 10 % DMSO in fetal bovine serum, and stored under −80 °C until testing.

2.3. Measurements of T-lymphocyte subtypes

Single cell suspensions were prepared from buffy coat with the use of a red blood cell lysis buffer (Biolegend). The following lymphocytes, i.e., NKT ($CD3^+CD56^+$), $CD4^+$ T, $CD8^+$ T, type 1 T helper (Th1) ($CD4^+CXCR3^+CCR6^-$), Th2 ($CD4^+CXCR3^-CCR6^-$), Th17 ($CD4^+CXCR3^-CCR6^+$), Treg ($CD4^+CD25^{high}CD127^{low}$), $CD25^+CD8^+$ T, $CD127^+CD8^+$ T, and NK ($CD56^+$) cells were detected using molecular specific antibodies, i.e., PerCP anti-human CD45, Alexa Fluor® 700 anti-human CD3, APC/Cyanine7 anti-human CD4, PE/Cyanine7 anti-human CD8, APC anti-human CD183 (CXCR3), PE anti-human CD56, PE/Dazzle™ 594 anti-human CD196 (CCR6), Brilliant Violet 421™ anti-human CD25, and Brilliant Violet 605™ anti-human CD127 (Biolegend). Dead cells were excluded using Zombie Aqua™ Fixable Viability Kit (Biolegend). APC Mouse IgG1, PE Mouse IgG1, PE/Dazzle™ 594 Mouse IgG2b, BV 421™ Mouse IgG1, and BV 605™ Mouse IgG1 were utilized as isotype control. The T cell subtypes were tested using BD LSR Fortessa flow cytometry and analyzed using FlowJo software (TreeStar). Representative T lymphocyte subtype plots are shown in Fig. 2.

2.4. Study outcome

The primary endpoint was treatment response which was assessed according to modified Response Evaluation Criteria in Solid Tumors (mRECIST, version 1.1) at 6 months after IO.[15] complete response (CR) on mRECIST was defined as disappearance of any intratumoral arterial enhancement in the target lesion. Surveillance imaging (contrast-enhanced magnetic resonance imaging [MRI] of the liver) was performed every 3 months, and patients with objective response (complete or partial response) were identified as responders, while others as non-responders. No pseudo-progression was identified, thus, the results of mRECIST should be similar to that of iRECIST, though iRECIST data was not collected. Progression-free survival (PFS) and overall survival (OS) were also reported, calculated from the start of TACE.

2.5. Statistical consideration

For small-sized longitudinal data with missing values, generalized estimation equation (GEE) was employed to test 1) changes of immune cells with time in all patients (main effect of time); 2) changes of immune cells with time in responders and non-responders (simple effect of time); and 3) differences of immune cells in responders and non-responders at different timepoints (simple effect of response). Bonferroni adjustment was performed for multiple testing. Comparisons between groups were determined by independent *t*-test, or one-way ANOVA followed by Tukey's multiple comparison tests, as appropriate. Results were expressed as mean (95% confidence interval [CI]). Statistical analyses and plots were conducted by SPSS 26.0 (IBM, Inc.) and GraphPad Prism (version 8), respectively.

3. Results

3.1. Patients and baseline STIE cells

A total of 35 patients were prospectively enrolled in the prospective biomarker study (GCOG0001/NCT05061342). The two cohorts were separated by time to approximate a ratio of 2:1 for exploratory (n = 23) and validation (n = 12) cohorts. All patients in the exploratory cohort were from the START-FIT trial, with characteristics reported previously.[14] Briefly, most of the patients recruited were male (22 male, 1 female) and had Child–Pugh class A. Fourteen (61 %) patients had *Hepatitis B* virus infection and 3 (13 %) had *Hepatitis C* virus infection. Fourteen (61 %) patients had Barcelona Clinic Liver Cancer (BCLC) stage C disease with macrovascular invasion and the mean tumor size was 10.0 (95 % CI: 5.3–17.5) cm. Baseline STIE cells in these patients showed remarkable heterogeneity but with no significant correlation with treatment responses in this series (Fig. 3).

3.2. Treatment induced changes in STIE cells

STIE cells changed significantly differentially after TACE, SBRT, and IO (Fig. 3). On average, the counts of leukocytes (Fig. 3A), lymphocytes (Fig. 3B), monocytes (Fig. 3C), and platelets (Fig. 3D) increased after TACE, decreased after SBRT, and then increased after IO, with the most notable changes in lymphocytes after SBRT. The mean lymphocyte counts increased by 0.4×10^9/L (95 % CI: 0.2×10^9/L–0.6×10^9/L, $P < 0.001$) after TACE, then decreased by 0.8×10^9/L (95 % CI: 0.5×10^9/L–1.1×10^9/L, $P < 0.001$) after SBRT, while restored by 0.4×10^9/L (95 % CI: 0.2×10^9/L–0.6×10^9/L, $P < 0.001$) after inducing IO (Fig. 3B). The mean monocyte counts increased after TACE-SBRT-IO by 0.2×10^9/L (95 % CI: 0.1×10^9/L–0.3×10^9/L, $P < 0.001$) (Fig. 3C). The mean platelet counts of all patients increased by 55.0×10^9/L (95 % CI: 16.9×10^9/L–93.0×10^9/L, $P = 0.001$) post-TACE, then displayed a reduction by 102.0×10^9/L (95 % CI: 48.1×10^9/L–155.1×10^9/L, $P < 0.001$) after receiving SBRT, and large number of reductions occurred primarily from one patient (Fig. 3D). There were no significant differences in treatment induced changes in any of these cells including lymphocytes, platelets, and monocytes between responders and non-responders in this cohort (Fig. 3).

3.3. Validating the STIE cell reshaping from TACE, SBRT, and IO

All patients in the validation cohort were male with a mean age of 64 (range: 50–75) years, and detailed characteristics are shown in Table 1. The mean tumor size (the largest diameter of the biggest lesion) was 8.4 (95 % CI: 6.1–10.7) cm. After IO treatment, six patients (50 %) had objective complete response. Representative MRI images of a patient with objective complete response were shown in Fig. 4.

3.4. Treatment induced changes in STIE cells in the validation cohort

Patients in the validation cohort also had STIE cells changed heterogeneously after TACE-SBRT-IO (Fig. 5), with a similar pattern of change to that of the exploratory cohort shown in Fig. 3. Lymphocytes (Fig. 5B) and platelets (Fig. 5D) decreased after SBRT, and then restored after IO, with nadirs observed after SBRT in almost all patients. The mean lymphocyte counts exhibited no significant changes after TACE, but a reduction by 0.7×10^9/L (95 % CI: 0.3×10^9/L–1.0×10^9/L, $P < 0.001$) after SBRT, and then increased by 0.4×10^9/L (95 % CI: 0.1×10^9/L–0.7×10^9/L, $P = 0.010$) after introduction of IO (Fig. 5B). The mean count of platelets increased by 70.4×10^9/L (95 % CI: 7.9×10^9/L–133.0×10^9/L, $P = 0.018$) post-TACE, and then decreased by 94.0×10^9/L (29.4×10^9/L–158.6×10^9/L, $P = 0.001$) after receiving SBRT (Fig. 5D). There were no significant treatment-induced changes in other cells tested, as shown in Fig. 5A, 5C, 5E, 5F, and 5G for leukocytes, monocytes, neutrophils, eosinophils, and basophils, respectively.

3.5. STIE cell changes and treatment responses in the validation cohort

All patents exhibited a reduction in lymphocytes after SBRT, with non-responders reducing more significantly (0.8×10^9/L, 95 % CI: 0.4×10^9/L–1.3×10^9/L, $P < 0.001$) than that of responders

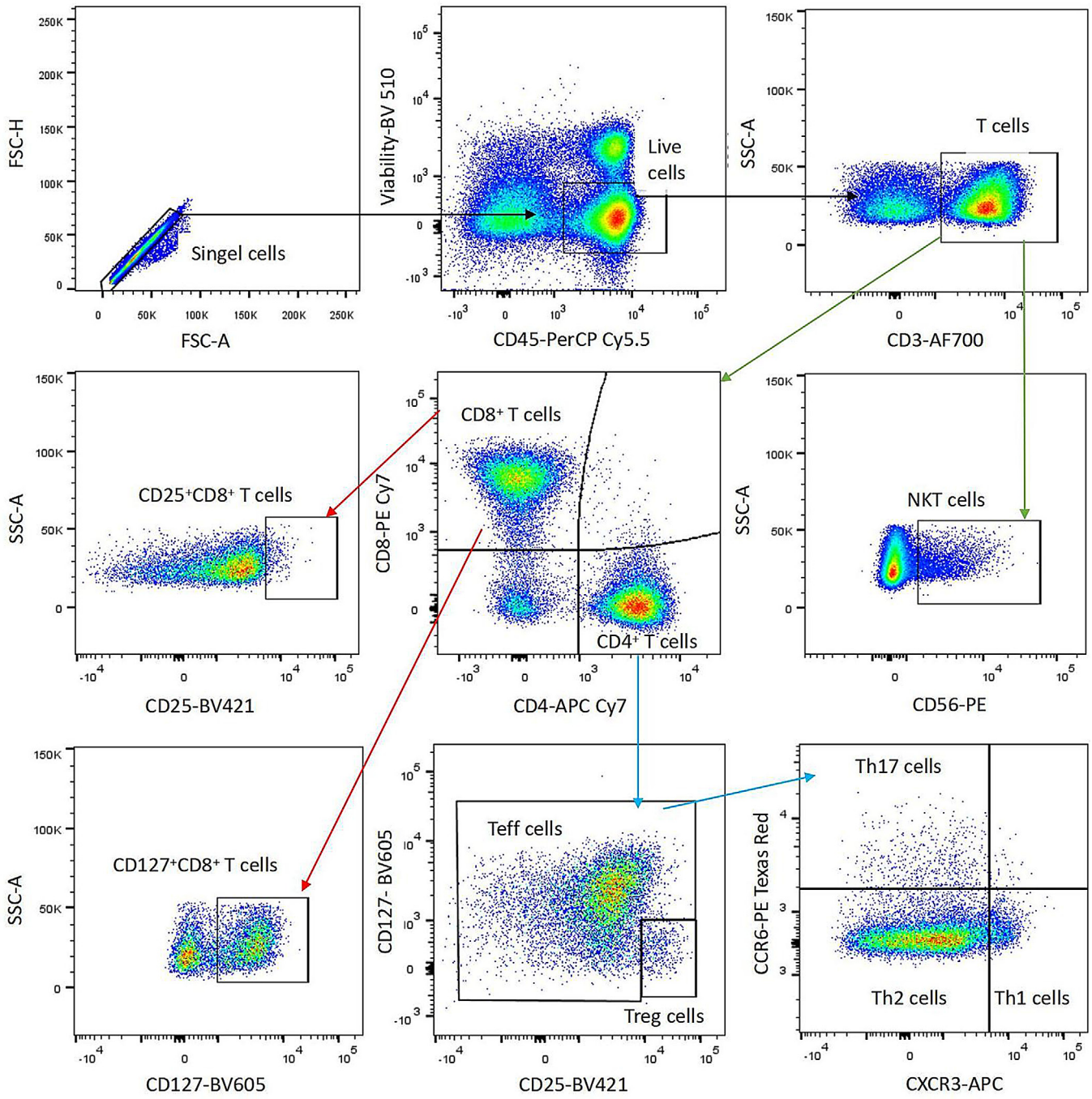

Fig. 2. Hierarchical gating strategy for T lymphocyte lineage. Initial gating in black lines was performed FSC-A vs. FSC-H to remove doublets; on CD45 and viability to gate live cells. Total T cells were separated from the live cells by expression of CD3. Subsequent gating in green lines of $CD3^+$ T cells identified T cell subsets, $CD4^+$ T, $CD8^+$ T, and NKT cells. $CD8^+$ T cell activation status was determined by the expression of CD25 and CD127 (red lines). For $CD4^+$ T cell subsets (blue lines), Treg cells were identified by expressions of high CD25 and low CD127, and then Th1, Th2, and Th17 cells were identified using CCR6 and CXCR3 expressions in Teff cell population. FSC-A, forward scatter area; FSC-H, forward scatter height; SSC-A, side scatter area; NKT cell, natural killer cell; Treg cell, regulatory T cell; Th cell, T helper cell; Teff, effector T cell.

(0.5×10^9/L, 95 % CI: 0.1×10^9/L–0.8×10^9/L, $P = 0.011$) (Fig. 5B). The responders demonstrated a significant increase in their absolute counts of lymphocytes, by an average of 0.3×10^9/L (95 % CI: 0.1×10^9/L–0.5×10^9/L, $P < 0.001$) after inducing IO (Fig. 5B). Besides, the responders' monocytes increased by 0.12×10^9/L (95 % CI: 0.06×10^9/L–0.17×10^9/L, $P < 0.001$) in mean counts after TACE-SBRT-IO (Fig. 5C). The non-responders had a significant reduction by 103.7×10^9/L (95 % CI: 9.7×10^9/L–197.7×10^9/L, $P = 0.022$) in the absolute counts of platelets after SBRT (Fig. 5D).

3.6. T-lymphocyte lineage

3.6.1. Baseline T-lymphocyte lineage in responders and non-responders

T-lymphocyte lineage detection was performed in the validation cohort. The baseline levels of T-lymphocyte lineage were heterogenous

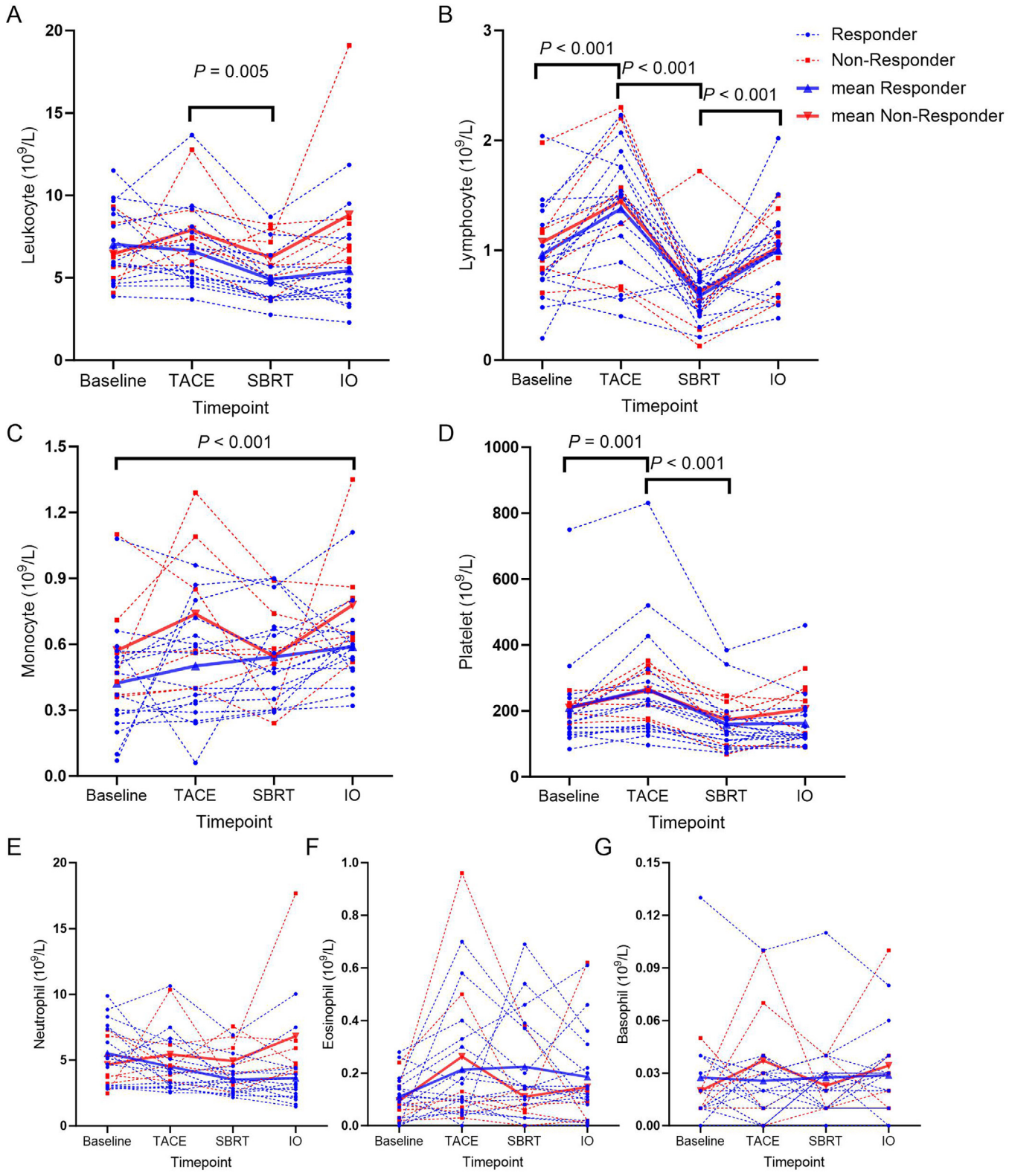

Fig. 3. Changes in STIE cells and treatment response in the 23 patients in the exploratory cohort. Absolute values of leukocyte (A), lymphocyte (B), monocyte (C), platelet (D), neutrophil (E), eosinophil (F) and basophil (G) of responders and non-responders at baseline, after TACE, SBRT and IO. The spaghetti plots show circulating complete blood cell counts at four timepoints; generalized estimation equation was used for significance verification. *P* values of all patients are shown on the top of plots. IO, immunotherapy; SBRT, stereotactic body radiotherapy; TACE, transarterial chemoembolization.

Table 1
Patient and tumor characteristics in the validation set.

Patient ID	History of *Hepatitis*	ECOG PS	CP score	BCLC stage	No. of tumors	Tumor size, cm[a]	Intra-hepatic vascular invasion	Response	PFS, months	OS, months
1	HCV	1	A5	C	3	8.2	RHV, MHV	PD	3	11
2	HBV	1	A5	B	2	4.3	No	CR	18+	18+
3	HBV	1	A5	C	1	11.9	MHV	CR	18+	18+
4	HBV	0	A5	C	2	6.7	MHV, LHV	SD	10	16+
5	HBV	1	A6	C	3	9.2	RHV, MHV	PD	2	2
6	HBV	0	A5	C	2	4.5	MHV	CR	16+	16+
7	HBV	1	A5	A	1	4.0	No	CR	15+	15+
8	HBV	1	A5	C	1	8.4	RPV	PD	2	6
9	HBV	1	A5	C	1	6.4	RHV, MHV, RPV	CR	13+	13+
10	HBV	1	A6	C	1	15.4	RHV	PD	2	12+
11	HBV	1	A5	C	1	13.6	MHV	CR	11+	11+
12	HBV	0	A5	C	1	8.2	RPV	PD	5	9+

[a] The largest diameter of the biggest lesion.
Abbreviations: BCLC stage, Barcelona clinic liver cancer stage; CP score, Child Pugh score; CR, complete response; ECOG PS, Eastern Cooperative Oncology Group Performance Status; LHV, left hepatic vein; MHV, middle hepatic vein; OS, overall survival; PD, progressive disease; PFS, progression free survival; RHV, right hepatic vein; RPV, right portal vein.

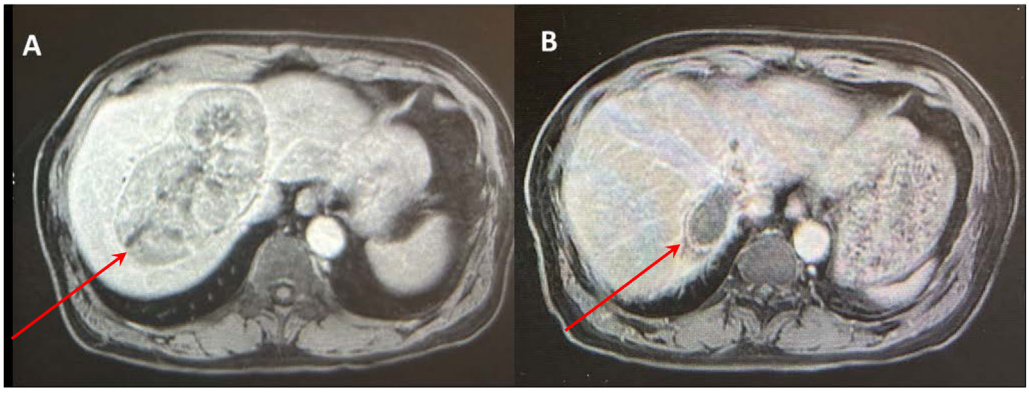

Fig. 4. Representative images of a responder. Images of patient#11 at baseline (A) and post-treatment (B). Red arrows indicate the tumor mass.

(Fig. 6A, E, F). The mean proportions of $CD8^+$ and $CD4^+$ T cells were 31.1 % (95 % CI: 19.2 %–43.1 %) and 57.7 % (95 % CI: 48.4 %–67.1 %), respectively. The $CD4^+$ T cells, Th1 cells, and Th1/Th17 ratios were significantly higher in responders (responders/non-responders: 63.0 %/49.0 %, $P = 0.010$; 19.7 %/8.3 %, $P = 0.007$; 9.3/1.7, $P = 0.001$, respectively), while $CD25^+CD8^+$ T cells, $CD127^+CD8^+$ T cells, Th17 cells, Treg cells, and Th2/Th1 ratios were significantly higher in non-responders (responders/non-responders: 4.0 %/16.3 %, $P < 0.001$; 44.3 %/64.8 %, $P = 0.003$; 3.1 %/6.4 %, $P = 0.047$; 3.7 %/6.6 %, $P = 0.002$; 5.0/11.3, $P = 0.028$, respectively). Representative plots illustrating the gating of the significant T cell lineage for both a responder and a non-responder are displayed in Fig. 6B-D, G, H.

3.6.2. *Treatment induced changing dynamics in T-lymphocyte lineage*

The dynamics in T-lymphocyte lineage, longitudinally from baseline to the end of TACE-SBRT- IO, are shown in Fig. 7. The average proportions of STIE $CD8^+$ T cells increased by 14.4 % (95 % CI: 2.3 %–26.5 %, $P = 0.010$) (Fig. 7A), while $CD4^+$ T cells decreased by 13.0 % (95 % CI: 2.8 % –23.3 %, $P = 0.005$) (Fig. 7B). The mean CD4/CD8 ratios (1.3, 95 % CI: 0.2 –2.4, $P = 0.008$) (Fig. 7C), and $CD127^+CD8^+$ T cells (30.5%, 95 % CI: 15.7%–45.3%, $P < 0.001$) (Fig. 7E) decreased significantly at the end of TACE-SBRT-IO.

3.6.3. *T-lymphocyte lineage changes in responders and non-responders*

The mean count of $CD127^+CD8^+$ T cells decreased significantly after TACE-SBRT-IO by 12.3% (95% CI: 9.3 %–29.2 %, $P < 0.001$) in responders but more remarkably by 49.2% (95% CI: 31.7%–66.7%, $P < 0.001$) in non-responders (Fig. 7E). The proportion of activated $CD25^+CD8^+$ T cells declined significantly only in non-responders after TACE and SBRT (Fig. 7D). The proportions of Th1, Th2, Th17, Treg, Th17/Treg, Th2/Th1, and Th1/Th17 changed numerically at different timepoints; however, they did not reach the level of statistical significance (Fig. 7F-L). There were no significant differences between responders and non-responders in other cells examined.

3.6.4. *STIE NKT cells and treatment response*

There were significant differences in the dynamic changes of NKT cells longitudinally from baseline to post-TACE-SBRT-IO, between responders and non-responders, with significantly higher NKT cells in the responders after SBRT in comparison to that of the non-responders (10.4% vs. 3.4%, $P = 0.001$) (Fig. 8A). The mean NKT cells increased after SBRT (from 6.9% to 10.4%) in responders, while it decreased in non-responders after SBRT. Representative plots illustrating the gating of the significant NKT cells for both a responder and a non-responder are displayed in Fig. 8B.

3.7. *SBRT dose and post-SBRT lymphocyte reduction*

The correlation between SBRT dose distribution and lymphocyte decease was analyzed in total 35 patients. There were 4 dose groups (27.5, 30, 35 and 40 Gy), and prescribed to 7, 16, 7, 5 patients, respectively. The mean reduction of lymphocytes (post-SBRT versus post-TACE) in these 4 groups were 0.6 ± 0.4, 0.7 ± 0.7, 0.7 ± 0.3 and $1.2 \pm 0.4 \times 10^9$/L, respectively. The differences of lymphocyte deceases were compared among groups, but with no significant correlation observed ($P = 0.218$) (Fig. 9A). However, the 40 Gy group appeared to have more reduction

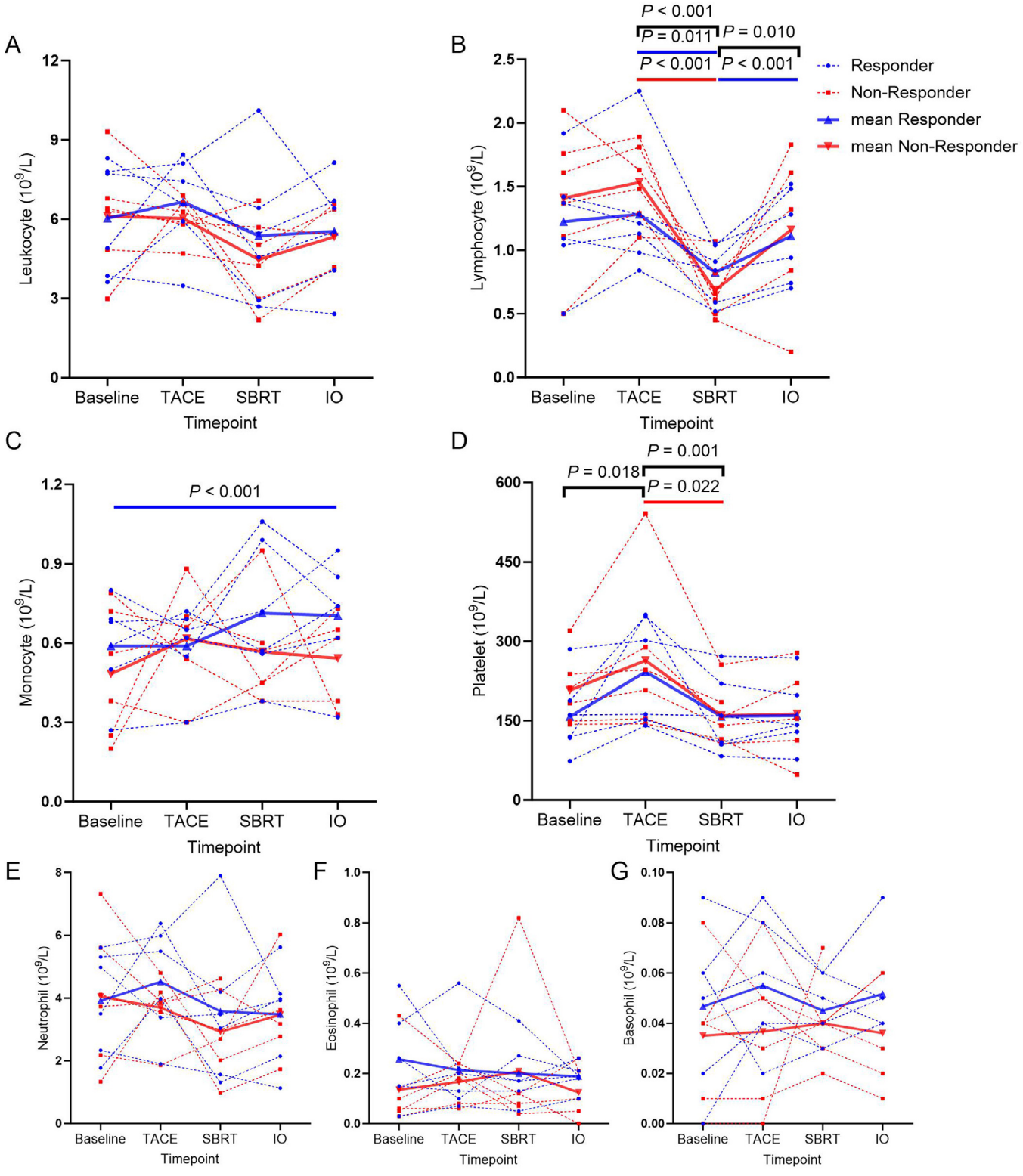

Fig. 5. Changes in STIE cells and treatment response in the 12 patients of the validation cohort. Absolute values of leukocyte (A), lymphocyte (B), monocyte (C), platelet (D), neutrophil (E), eosinophil (F) and basophil (G) of responders and non-responders at baseline, after TACE, SBRT and IO. The spaghetti plots show circulating complete blood cell counts at four timepoints; generalized estimation equation was used for significance verification. *P* values are shown on the top of plots. Black, all patents; blue, responders; red, non-responders. IO, immunotherapy; SBRT, stereotactic body radiotherapy; TACE, transarterial chemoembolization.

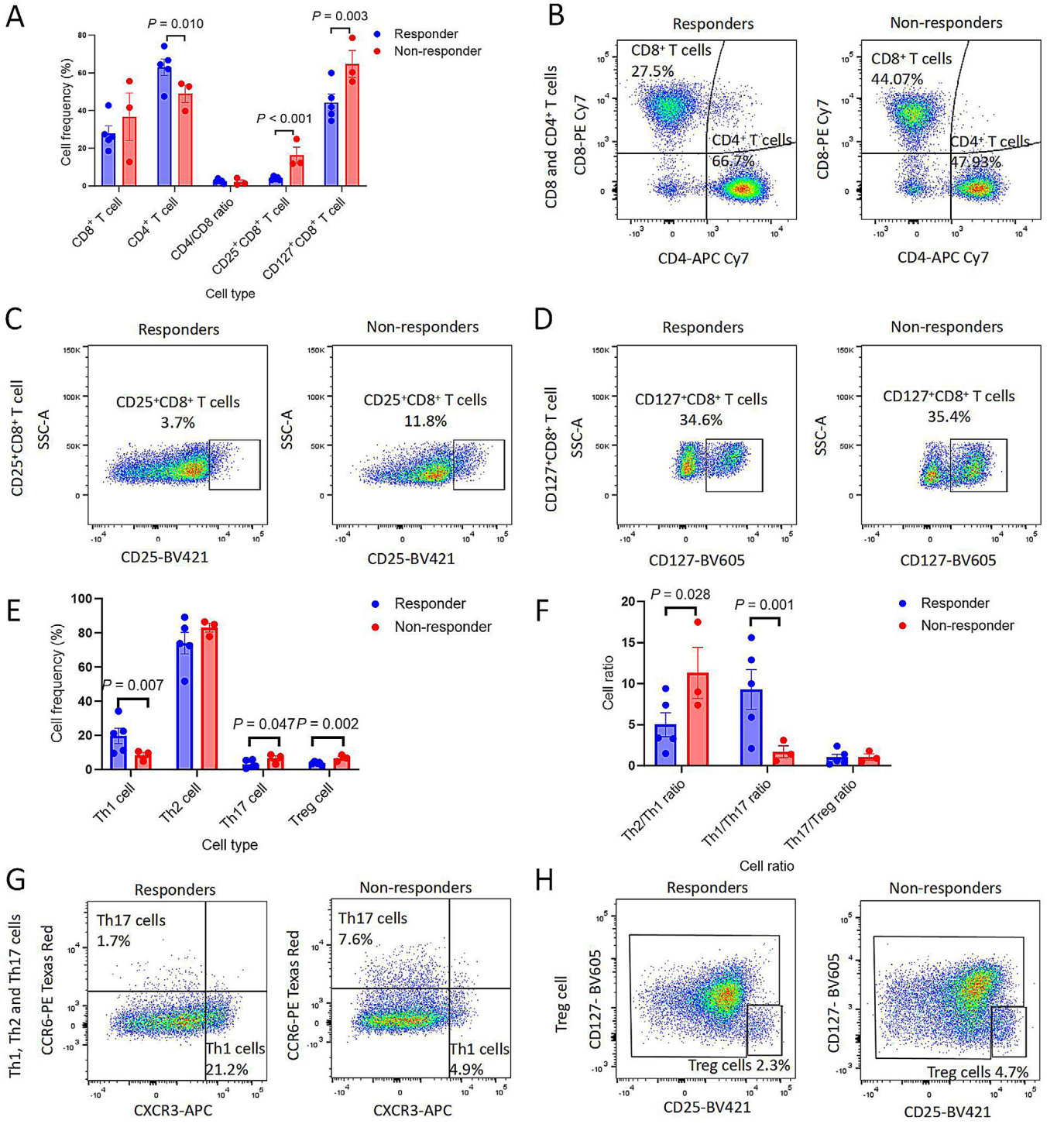

Fig. 6. Baseline STIE T-lymphocyte lineage and treatment responses. (A) $CD8^+$ T cell, $CD4^+$ T cell, CD4/CD8 ratio, $CD25^+CD8^+$ T cell, $CD127^+CD8^+$ T cell and treatment responses (responder, blue; non-responder, red); representative plots showing the gating of (B) $CD8^+$ T, $CD4^+$ T, (C) $CD25^+CD8^+$ T, (D) $CD127^+CD8^+$ T cells from responders or non-responders; (E) Th1, Th2, Th17 and Treg cells, (F) Th2/Th1, Th1/Th17 and Th17/Treg ratios and treatment response (responder, blue; non-responder, red). Representative plots showing the gating of (G) Th1, Th2, Th17 and (H) Treg cells from responders (left) or non-responders (right). The bar shows individual, mean, and standard error of mean. Independent *t*-test was used for significance verification.

than those of lower dose groups ($P = 0.037$). Moreover, the relationship between post-SBRT absolute lymphocyte count (ALC) and SBRT dose distribution was also explored. The mean post-SBRT ALCs in the 4 dose groups were 0.6 ± 0.3, 0.7 ± 0.3, 0.5 ± 0.2, and $0.7 \pm 0.2 \times 10^9$/L, respectively, but there was no significant difference among these 4 groups ($P = 0.751$) (Fig. 9B).

4. Discussion

This study demonstrated that the baseline STIE cells were heterogenous in locally advanced unresectable HCC, and immune stimulating cells including $CD4^+$ T and Th1 cells were significantly higher in responders, while Th17 and Treg cells were higher in non-responders. Af-

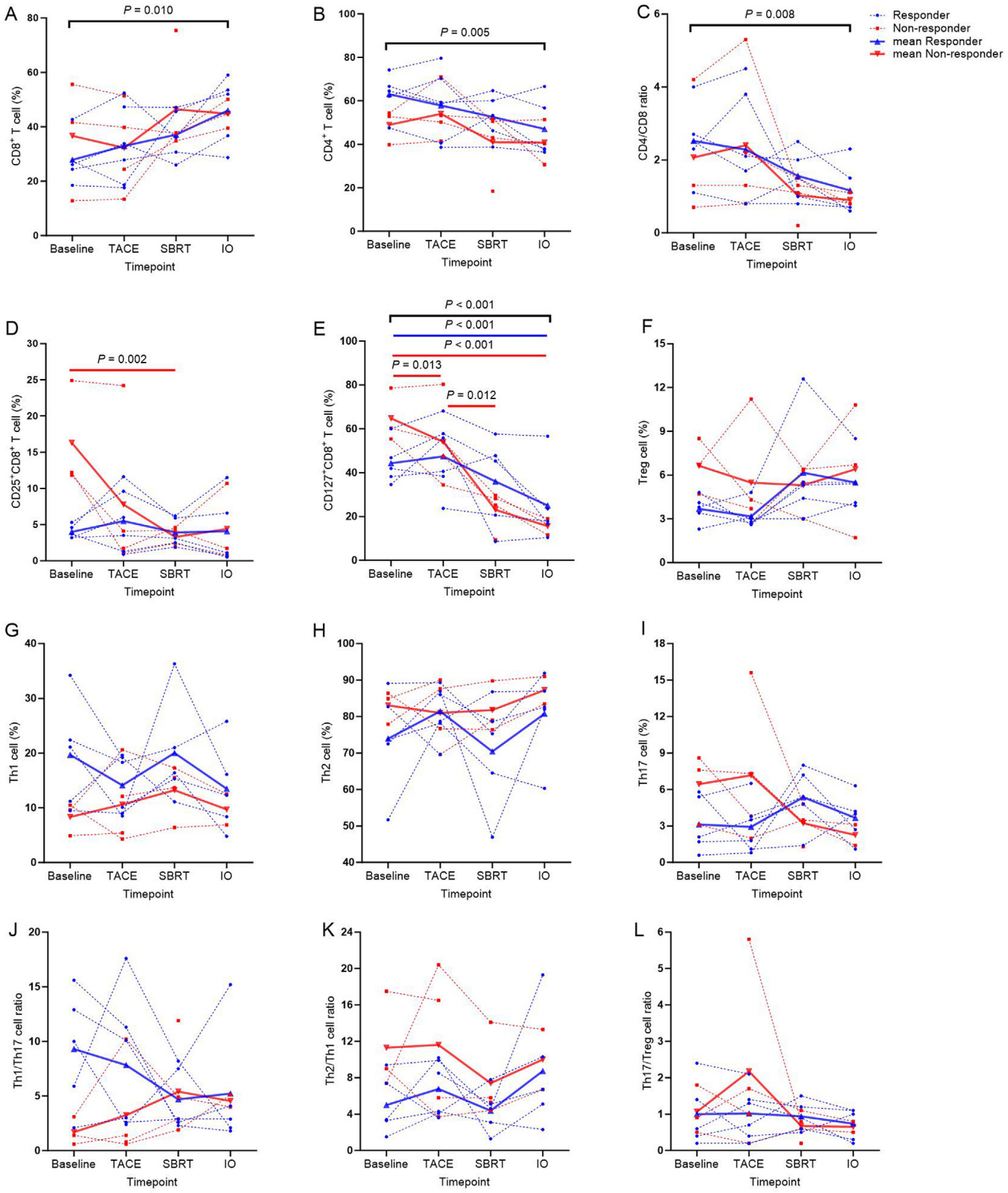

Fig. 7. Changes in STIE T-lymphocyte lineage and treatment responses. This figure shows overall changes of T-lymphocyte in each patient and average of responders and non-responders. The spaghetti plots show circulating T-lymphocyte lineages at four timepoints of all patients, including $CD8^+$ T cell (A), $CD4^+$ T cells (B), CD4/CD8 ratio (C), $CD25^+CD8^+$ T cell (D), $CD127^+CD8^+$ T cell (E), Treg cell (F), Th1 cell (G), Th2 cell (H), Th17 cell (I), Th1/Th17 ratio (J), Th2/Th1 ratio (K), and Th17/Treg ratio (L) after TACE, SBRT and IO. Generalized estimation equation was used for significance verification. Black, all patents; blue, responders; red, non-responders. IO, immunotherapy; SBRT, stereotactic body radiotherapy; TACE, transarterial chemoembolization.

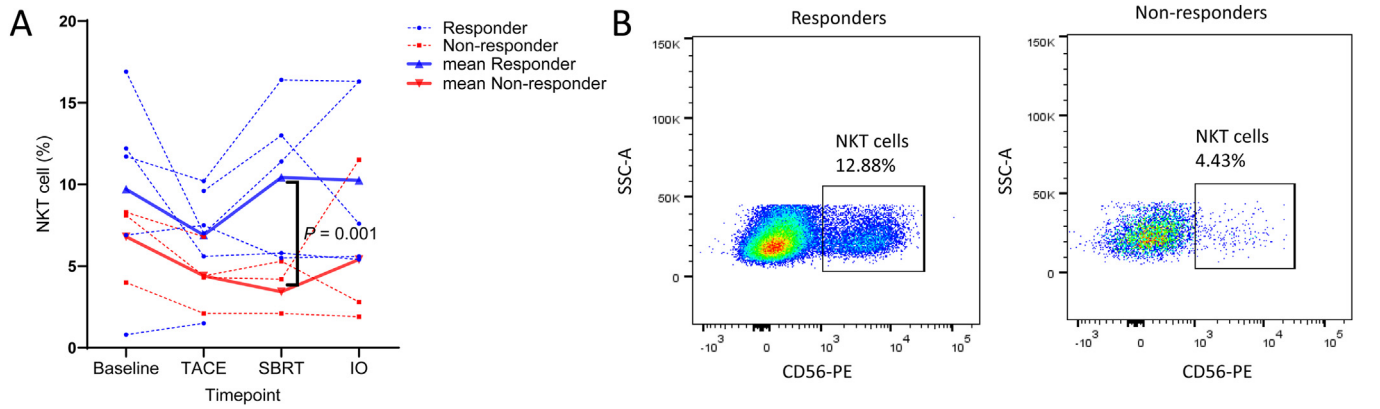

Fig. 8. Changes in STIE NKT cells and treatment response. This figure shows the overall changes of NKT cells in each patient and the average of responders and non-responders. (A) Proportions of post-SBRT NKT cells in responders and non-responders at baseline, after TACE, SBRT and IO. The spaghetti plots show NKT cells at four timepoints of all patients, and generalized estimation equation was used for significance verification. (B) Representative plots showing the gating of NKT cells from responders (left) or non-responders (right). IO, immunotherapy; SBRT, stereotactic body radiotherapy; TACE, transarterial chemoembolization.

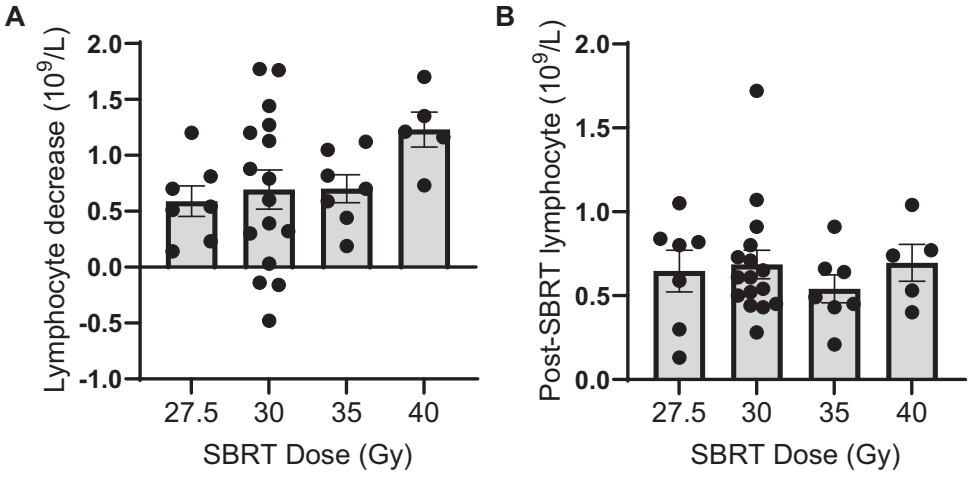

Fig. 9. SBRT dose and post-SBRT lymphocyte reduction. This figure maps (A) post-SBRT lymphocyte reduction and (B) post-SBRT absolute lymphocyte count with SBRT dose distribution in all patients with hepatocellular carcinoma. The bar shows individual, mean and standard error of mean. One-way ANOVA followed by Tukey's multiple comparison test was used for significance verification. SBRT, stereotactic body radiotherapy.

ter treatment with TACE, SBRT, and IO, STIE cells and T-lymphocyte lineage changed differentially: there were significant reductions after TACE and SBRT in $CD25^+CD8^+$ T and $CD127^+CD8^+$ T cells in non-responders, while increases in NKT cells after SBRT and total lymphocytes during IO were seen in responders. This is a STIE circulating biomarker study for a unique multimodality regimen of the START-FIT (NCT03817736, recently reported in *Lancet Gastroenterol Hepatol*) with 3 treatment modalities of TACE-SBRT-IO in each patient with locally advanced unresectable HCC.[14]

Our new finding was that $CD4^+$ T cells, Th1 cells, Th1/Th17 ratio, Th17 cells, Th2/Th1 ratio, and Treg cells had differential effects on the treatment responses to TACE-SBRT-IO, though the heterogeneity of STIE circulating cell distribution has been previously reported.[16] From the immunobiology point of view, $CD4^+$ T cells, Th1 cells, and Th1/Th17 ratio are known for their positive immune stimulation effect, while Th2/Th1 ratio and Treg cells are immune suppressive. For example, $CD4^+$ T cells are associated with good treatment response, as these cells can help the immune response by stimulating other immune cells, such as macrophages, to eliminate cancer cells. The role of Th1 and its balance with Th17 in both TME and STIE were reported to have association with PFS and OS in HCC patients following surgical resection.[17] Indeed, Th17 cells play a crucial role as a component of adaptive immunity and have diverse functions, particularly in inflammation and tissue protection. They make important contributions, especially in mucosal reactions, to host defense against extracellular pathogens. However, in HCC patients, proinflammatory Th17 cells have been reported to accumulate in HCC tissue, where they promote disease progression by fostering angiogenesis and are negatively correlated with Th1 cells.[17,18] Our findings of higher proportions of Th1 cells in responders and higher levels of Th17 in non-responders are consistent with previous reports.[17-20] Similarly, Treg cells were associated with poor response to the treatment as expected since Treg cells promote an immunosuppressive microenvironment to suppress anti-tumor immune effector responses.[21,22] It is hard to understand, however, that the baseline levels of $CD127^+CD8^+$ T cells and $CD25^+CD8^+$ T cells were significantly associated with poor response (Fig. 7). CD127 appears to be a marker of effector memory T cell phenotype. $CD25^+CD8^+$ T cells are known as the activated phenotype of $CD8^+$ T cells, and it is positively correlated with improved OS in HCC patients treated with hypofractionated radiation therapy.[12,23,24] Further subtyping analysis may help understand the underlying biological rationale. One possibility could be the vulnerability of these cells to treatment damage and importance of their levels at the time of SBRT and IO treatment instead of baseline. Indeed, both $CD25^+$ and $CD127^+CD8^+$ T cells decreased significantly after TACE and SBRT; the non-responders, though started with more of these cells, had similar or lower levels at the end of IO treatment, suggesting the importance of the cells at the time of SBRT and IO delivery.

The STIE cells changed heterogeneously after sequential TACE, SBRT, and IO in the same patient and SBRT induced the most significant reductions in lymphocytes and platelets among the three modali-

ties, observed in both the exploratory and validation sets. It is also interesting to note that the $CD25^+$ and $CD127^+CD8^+$ T cells reduced significantly after SBRT. More reduction of immune effective lymphocytes in non-responders indicate more radiation immune suppression likely from high sensitivity to radiation damage or high dose exposure of the STIE. Future studies on radiosensitivity of $CD25^+CD8^+$ T cells and $CD127^+CD8^+$ T-lymphocytes may also help guide precision immunotherapy. As high doses were associated with better responses, the dose of SBRT should be determined such that the dose ratio of tumor versus the STIE are maximized in each patient.

It is worth noting that the immunomodulatory effect of SBRT has been an important topic, but with limited evidence from patients. On the one hand, radiation-induced lymphopenia has been reported to associate with worse outcomes in HCC patients, which is in concordance with findings in this study.[25] On the other hand, radiotherapy could induce immunogenic cell death as a "vaccine" and increase the diversity and clonality of intra-tumoral T cell receptor (TCR) repertoire.[26] SBRT significantly decreased the number of lymphocytes and cytotoxic $CD8^+$ T cells in STIE, suggesting a possible immune inhibitory effect in the circulation blood. Less reduction association with better response suggests the importance of high-precision immune preserving radiation technology.

It is intriguing to see the dynamics of NKT cells, which increased after the treatment modality of TACE, SBRT, and IO in the responders, and had elevated significantly more after the treatment of SBRT (from 6.9% to 10.4%). NTK cells, a special subset of T cells with both T cell receptors (TCR) and NK cell receptors on the cell surface, are particularly known to play an important role in HCC progression.[27] NKT cells can produce large quantities of cytokines and exert cytotoxic effects similar to those of NK cells, but are also equipped with the immunomodulatory function of T cells.[11] The number of post-SBRT NKT cells was positively associated with improved response in the present study, suggesting SBRT triggered NKT cell expansion in the responders. This finding is in line with previous reports in the literature. For instance, Li et al. demonstrated that the peripheral NKT cells increased post-SBRT and patients with higher levels of NKT cells achieved higher 2-year OS.[11] Further validation study with a large sample size is warranted for the role of NKT cells as a biomarker of SBRT immune stimulation and possible targeted cell immunotherapy.

It is important to note that this study, for the first time to our knowledge, reported differential changes of STIE cells after TACE, SBRT, and IO in the same patient. Most of reports, however, were either from animal studies or small series of single-modality treatments,[9-13] which cannot compare the differential effects from various modalities in the same patient and do not meet the need of the current standard care of combined multi-modality treatments. One study by Tang et al. reported the significance of two modalities. According to the study, an increased level of circulating $CD8^+$ T cells, CD8/CD4 ratio, and $CD8^+$ T cells expressing 4–1BB and PD1 denoted responses in patients receiving a combination of ipilimumab and SBRT to liver or lung lesions.[28] Knowledge is much coveted, especially in an individual for his or her responses to various modalities.[29] If validated externally, our significant findings on STIE circulating cells and longitudinal changes during TACE-SBRT-IO treatment would shed light to promote more STIE based research on this deadly disease, suggesting the potential of using STIE to guide future personalized immunotherapy to improve the treatment outcome.

While the findings of this study are innovative and have significant clinical implication, one has to note that this study is limited in sample size. Significant results from small sample sized study could be a result of random effects from testing or remarkable magnitude of difference in a specifically enriched study population. Our results of STIE immune cells were validated in an independent dataset, and we applied GEE testing for stringent correction. The significant results from this study are most likely due to highly selected study populations consisting only of patients with large unresectable HCC, uniform treatment modalities, and strictly time-controlled TACE-SBRT-IO in all subjects. For the example of the treatment effects on STIE, there was no individual confounding variables as comparison was between post- and pre-treatment in the same patient. We thus believe the finding from this small-sized study is at least partially hypothesis proving.

In summary, this study mapped STIE circulating cells after sequential TACE, SBRT, and IO in unresectable HCC, revealed heterogenous and significant changes in lymphocytes and T-lymphocyte lineage and their relationship with tumor control at 6 months post-IO. Findings of this study suggest the role of host STIE cells and the more reshaping effect of SBRT. It is interesting to note that high levels of $CD4^+$ T cells, Th1 cells, and high ratios of Th1/Th17 at baseline and SBRT induced increase in NKT cells were significantly higher in responders, while baseline levels of Treg cells, Th17 cells, Th2/Th1 ratio were significantly associated with poor response after TACE-SBRT-IO treatment. This finding is potentially useful because we could predict treatment response after TACE-SBRT-IO multi-modality regimen according to baseline and changes of STIE levels, and thus have the opportunity to adjust and optimize further therapies. Validation trials and further research on the role of STIE T-lymphocytes on immunotherapy responses are warranted to better personalize treatment therapies.

Declaration of competing interest

The authors declare that they have no known competing financial interests or personal relationships that could have appeared to influence the work reported in this paper.

Ethics statement

This study was approved by the Institutional Review Boards of Queen Mary Hospital (approval number: UW 19-565). All of the study designs and test procedures were performed in accordance with the Helsinki Declaration ll. All patients signed the informed consent for specimen and meidcal data collection.

Consent for publication

The patients whose medical images are presented in this manuscript provided consentfor publication of their medical images for the manuscript. Only de-identified data andimages are used in this article.

Acknowledgments

We thank Dr. Zhi-Wu TAN from AIDS Institute and Department of Microbiology (The University of Hong Kong) for providing critical comments. We thank Dr. Sai-Kit LAM from Research Institute for Smart Ageing and Department of Biomedical Engineering (The Hong Kong Polytechnic University) for language polishing. We thank Emily LIU and Erica YAU from the Imaging and Flow Cytometry Core Centre for PanorOmic Sciences (The University of Hong Kong) for providing and maintaining the equipment and technical support needed for flow cytometry analysis. This study was supported by the Shenzhen Science and Technology Program (grant number: KQTD20180411185028798).

Author contributions

C.N.Z., C.L.C., C.Y.C., and F.M.K. provided study conception and design; C.L.C., S.K.C., C.B.L., and C.Y.C. recruited patients; W.H.C. performed response assessment; C.N.Z., W.W.C., and D.Y.Z. collected samples; C.N.Z. and F.M.K. performed data analysis and drafted manuscript; all other co-authors reviewed, edited, and approved the final manuscript.

References

1. Ma L, Wang L, Khatib SA, et al. Single-cell atlas of tumor cell evolution in response to therapy in hepatocellular carcinoma and intrahepatic cholangiocarcinoma. *J Hepatol*. 2021;75(6):1397–1408.

2. Xu L, Zou C, Zhang S, et al. Reshaping the systemic tumor immune environment (STIE) and tumor immune microenvironment (TIME) to enhance immunotherapy efficacy in solid tumors. *J Hematol Oncol*. 2022;15:87.
3. Wu TD, Madireddi S, de Almeida PE, et al. Peripheral T cell expansion predicts tumour infiltration and clinical response. *Nature*. 2020;579(7798):274–278.
4. Spitzer MH, Carmi Y, Reticker-Flynn NE, et al. Systemic immunity is required for effective cancer immunotherapy. *Cell*. 2017;168(3):487–502.
5. Zhong RB, Zhang YB, Chen DF, et al. Single-cell RNA sequencing reveals cellular and molecular immune profile in a Pembrolizumab-responsive PD-L1-negative lung cancer patient. *Cancer Immunol Immunother*. 2021;70(8):2261–2274.
6. De Biasi S, Gibellini L, Lo Tartaro D, et al. Circulating mucosal-associated invariant T cells identify patients responding to anti-PD-1 therapy. *Nat Commun*. 2021;12(1):1669.
7. Griffiths JI, Wallet P, Pflieger LT, et al. Circulating immune cell phenotype dynamics reflect the strength of tumor-immune cell interactions in patients during immunotherapy. *Proc Natl Acad Sci U S A*. 2020;117(27):16072–16082.
8. Krieg C, Nowicka M, Guglietta S, et al. High-dimensional single-cell analysis predicts response to anti-PD-1 immunotherapy. *Nat Med*. 2018;24(2):144–153.
9. Park H, Jung JH, Jung MK, et al. Effects of transarterial chemoembolization on regulatory T cell and its subpopulations in patients with hepatocellular carcinoma. *Hepatol Int*. 2020;14(2):249–258.
10. Li F, Guo Z, Lizee G, et al. Clinical prognostic value of CD4+CD25+FOXP3+regulatory T cells in peripheral blood of Barcelona Clinic Liver Cancer (BCLC) stage B hepatocellular carcinoma patients. *Clin Chem Lab Med*. 2014;52(9):1357–1365.
11. Li TT, Sun J, Wang Q, et al. The effects of stereotactic body radiotherapy on peripheral natural killer and CD3+CD56+ NKT-like cells in patients with hepatocellular carcinoma. *Hepatob Pancreatic Dis Int*. 2021;20(3):240–250.
12. Grassberger C, Hong T, Hato T, et al. Differential association between circulating lymphocyte populations with outcome after radiation therapy in subtypes of liver cancer. *Int J Radiat Oncol Biol Phys*. 2018;101(5):1222–1225.
13. Chew V, Lee YH, Pan L, et al. Immune activation underlies a sustained clinical response to Yttrium-90 radioembolisation in hepatocellular carcinoma. *Gut*. 2019;68(2):335–346.
14. Chiang CL, Chiu KWH, Chan KSK, et al. Sequential transarterial chemoembolisation and stereotactic body radiotherapy followed by immunotherapy as conversion therapy for patients with locally advanced, unresectable hepatocellular carcinoma (START-FIT): a single-arm, phase 2 trial. *Lancet Gastroenterol Hepatol*. 2023;8(2):169–178.
15. Lencioni R, Llovet JM. Modified RECIST (mRECIST) assessment for hepatocellular carcinoma. *Semin Liver Dis*. 2010;30(1):52–60.
16. Hung YP, Shao YY, Hsu C, et al. The unique characteristic in peripheral immune cells in patients with advanced hepatocellular carcinoma. *J Formos Med Assoc*. 2021;120(8):1581–1590.
17. Yan J, Liu XL, Xiao G, et al. Prevalence and clinical relevance of T-helper cells, Th17 and Th1, in hepatitis B virus-related hepatocellular carcinoma. *PLoS One*. 2014;9(5):e96080.
18. Kuang DM, Peng C, Zhao QY, et al. Activated monocytes in peritumoral stroma of hepatocellular carcinoma promote expansion of memory T helper 17 cells. *Hepatology*. 2010;51(1):154–164.
19. Zhang JP, Yan J, Xu J, et al. Increased intratumoral IL-17-producing cells survival in hepatocellular carcinoma correlate with poor patients. *J Hepatol*. 2009;50(5):980–989.
20. Liao R, Sun J, Wu H, et al. High expression of IL-17 and IL-17RE associate with poor prognosis of hepatocellular carcinoma. *J Exp Clin Cancer Res*. 2013;32(1):3.
21. Strauss L, Bergmann C, Whiteside TL. Functional and phenotypic characteristics of CD4+CD25highFoxp3+ Treg clones obtained from peripheral blood of patients with cancer. *Int J Cancer*. 2007;121(11):2473–2483.
22. Fu J, Xu D, Liu Z, et al. Increased regulatory T cells correlate with CD8 T-cell impairment and poor survival in hepatocellular carcinoma patients. *Gastroenterology*. 2007;132(7):2328–2339.
23. Crawley AM, Katz T, Parato K, et al. IL-2 receptor gamma chain cytokines differentially regulate human CD8+CD127+ and CD8+CD127- T cell division and susceptibility to apoptosis. *Int Immunol*. 2009;21(1):29–42.
24. Paiardini M, Cervasi B, Albrecht H, et al. Loss of CD127 expression defines an expansion of effector CD8+ T cells in HIV-infected individuals. *J Immunol*. 2005;174(5):2900–2909.
25. De B, Ng SP, Liu AY, et al. Radiation-associated lymphopenia and outcomes of patients with unresectable hepatocellular carcinoma treated with radiotherapy. *J Hepatocell Carcinoma*. 2021;8:57–69.
26. Twyman-Saint Victor C, Rech A, Maity A, et al. Radiation and dual checkpoint blockade activate non-redundant immune mechanisms in cancer. *Nature*. 2015;520(7547):373–377.
27. Sun C, Sun HY, Xiao WH, et al. Natural killer cell dysfunction in hepatocellular carcinoma and NK cell-based immunotherapy. *Acta Pharmacol Sin*. 2015;36:1191–1199.
28. Tang C, Welsh JW, de Groot P, et al. Ipilimumab with stereotactic ablative radiation therapy: phase I results and immunologic correlates from peripheral T cells. *Clin Cancer Res*. 2017;23(6):1388–1396.
29. Chiang CL, Chan ACY, Chiu KWH, et al. Combined stereotactic body radiotherapy and checkpoint inhibition in unresectable hepatocellular carcinoma: a potential synergistic treatment strategy. *Front Oncol*. 2019;9:1157.